Conceptual Design Study of High Field Magnets for Very Large Hadron Collider

G. Ambrosio (1), S. Caspi (2), V.V. Kashikhin (1), P.J. Limon (1),

T. Ogitsu (3), I. Terechkine (1), M. Wake (3), R. Yamada (1), A.V. Zlobin (1)

***Abstract*: - During the last year, Fermilab in collaboration with LBNL and KEK was conducting an extensive design study of superconducting magnet with a two-layer cosine-theta coil for a post-LHC hadron collider. For the 30-50 mm magnet bore range, different superconducting cable types, current block arrangements, and iron yoke outer diameters were considered. This paper summarizes results of the study including field and force distribution, systematic and random field error analysis, and coil magnetization and iron saturation effects.**

I. INTRODUCTION

One of the approaches to a post-LHC Very Large Hadron Collider (VLHC) is based on high field superconducting magnet [1]. Although operational field for this machine has yet to be determined, the 10-12 Tesla magnetic field range is now considered as being close to optimal. First, synchrotron radiation of a high-energy proton in this field provides sufficient amount of radiation damping that allows certain relaxation of magnet field quality requirements. Second, radiated power still can be removed with the help of a cold beam screen [2]. Development of a high field accelerator magnet with the operational magnetic field above 10 T based on the NbTi technology does not look feasible even at 1.8 K because of critical current and magnetic field limitations for this material.

Three Nb_3Sn short dipole magnets were built in the 90s that could exceed 10 T magnetic field. Table 1 below summarizes the main design parameters of those magnets [3-5]. All of the magnets were shell-type dipoles with bore diameter of 50 mm. Magnetic field gain was achieved in each next design by using thicker coil; this increased coil fabrication complexity. None of the magnets provided the accelerator field quality; building each of them was an attempt to show feasibility of a high-field Nb_3Sn magnet.

Gained experience and recent progress in the development of Nb_3Sn superconducting strand [6] has made it real building an accelerator-quality dipole magnet in the desired field range using a shell-type two-layer coil. Development of such a magnet and cost effective production technology would provide a solid base not only for the VLHC R&D work, but also for other high-field magnet applications.

(1) FNAL, Batavia, IL, (2) LBNL, Berkeley, CA, (3) KEK, Japan

Table 1. Superconducting Nb_3Sn Magnets.

Laboratory	CERN	UT	LBNL
Aperture (mm)	50	50	50
Coil type	Shell	Shell	Shell
Number of layers	2	2	4
Coil thickness (mm)	34	40	54
Bmax @4.3 K, (T)	10.0	11.5	13

This paper summarizes the results of the design study performed in the frame of R&D program at Fermilab in collaboration with LBNL and KEK. The goal of this study was to define a range of basic input parameters for the high field Nb_3Sn dipole magnetic design.

II. CROSS-SECTION DESIGN

There are several parameters that should be considered while developing a new superconducting magnet. Some of them are strand and cable characteristics, bore diameter, nominal field, field quality, forces developed in a coil during excitation cycle, iron yoke inner and outer diameter, stored energy, and coil inductance. In this study, characteristics of commercially available superconducting strand were used. The status of Nb_3Sn strand production technology can be found in [6]. IGC "internal tin" strand with critical current density of 1886 A/mm^2 at 12 T and 4.2 K was chosen for sample cable fabrication. Copper-to-noncopper ratio for the strand was about 0.85:1 with copper matrix purity parameter RRR=100. The parameters of the two types of cable used in this study are shown in table 2. For the purpose of this design study, cable insulation thickness was considered to be 0.125 mm all around the cable that corresponded to the commercially available S2-glass insulation or to the ceramic insulation recently developed at CTD company [7].

Table 2. Cable Parameters.

Parameter	Type 1	Type 2
Number of strands	28	38
Strand diameter [mm]	1.012	0.808
Radial width [mm]	14.232	15.400
Midthickness [mm]	1.800	1.456
Keystone angle [deg.]	1.0	0.5

There are several contradictory requirements that should be taken into account for making a choice of a magnet bore size. Large magnet bore helps to improve magnet field quality and magnetic measurement accuracy as well as to simplify beam screen design and coil end winding. Small magnet bore is beneficial for the stored energy, inductance, and mechanical stress reduction. It also helps to decrease coil mass and thus leads to magnet cost saving. Design and fabrication issues of a magnet production tooling are also very important for implementation of a practical magnet.

Next criteria were used to make preliminary cross-section choice:

- bore range from 30 to 50 mm,
- quench field is more then 12 T,
- field is of accelerator quality.

Pre-selected design versions were compared using such parameters as transfer function, stored energy, inductance, mechanical stress developed in coil during excitation, and some others. Also additional restrictions were used to simplify coil fabrication and to improve its reliability. Cables were required to be positioned as radially as it was possible. Inner-layer pole key width was restricted by 13 mm based on our previous coil winding experience and on the results of specially performed winding test. Besides, space between the two adjacent coil blocks ought to accommodate a sufficiently thick wedge.

Figure 1 shows the cable block arrangements for the four pre-selected cross-sections. Three of them shown in the quadrants I, II, and III use type 1 cable and have 50, 45 and 40 mm bore respectivelly. Cross-section shown in the quadrant IV uses type 2 cable and has 40 mm bore.

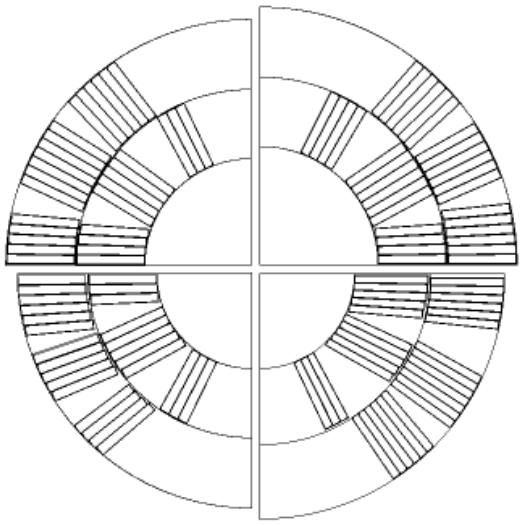

Fig. 1. Cross-section layout.

Dipole cross-sections with bore diameters less then 40 mm were also studied. It was possible to find 35 and 30 mm bore cross-sections with rather good field quality. Nevertheless, they were rejected because coil block distribution for these cross-sections implied some coil winding problems.

Based on preliminary results of mechanical and magnetic calculations, the 9-mm gap between the coil and the yoke was chosen. It resulted in the inner diameter of the iron yoke of 120 mm for the 40-mm bore diameter case, 121 mm for the 45 mm bore, and 126.5 mm for the 50 mm bore.

III. CROSS-SECTION ANALYSIS

At the first stage of this study, no iron saturation effects were considered. ROXIE superconducting magnet optimization code [8] was used to generate and to analyze cross-sections. Table 3 presents major parameters of the four designs: bore diameter, number of turns, maximum central field Bss, short sample limit Iss, current Inom corresponding to the 11 T central field, stored energy at 11 T, magnet inductance, coil area, and inner-layer pole width. As it can be seen, the maximum central field exceeds 12 T level for all the four designs. While number of turns drops from 32 to 26 by 20% as bore diameter reduces, current increase is only 9%. Stored energy becomes smaller by 25% and inductance decrease is 35%. Significant saving of superconductor material is possible if to choose smaller magnet bore diameter. Pole width and cable block positioning for every of the four preselected designs insure potentially good cable windability.

Table 3. Magnet Design Comparison.

Cable type	Type 1			Type 2
Bore diam. (mm)	50	45	40	40
Turns per dipole	64	60	52	64
B/I (T/kA)	0.76	0.74	0.68	0.81
Bss (T)	12.4	12.4	12.5	12.5
Iss (kA)	16.8	16.8	18.5	15.4
Inom (kA)	14.5	14.9	16.2	13.5
Energy@11T (kJ/m)	289	256	221	230
Inductance (mH/m)	2.75	2.32	1.67	2.53
Coil area (cm^2)	33.0	30.1	26.6	28.7
Pole width (mm)	17.5	16.2	15.0	14.6

Table 4 summarizes the calculated Lorentz forces at 11 T. Since forces and stresses become smaller when coil diameter decreases, lower coil azimuthal prestress is required. For all the cases studied, radial component of coil stress was less than 60 MPa. The combination of radial and azimuthal stress gives maximum stress value in each of the coils of less than 100 MPa at 11 T.

Forces and streses in table 4 were obtained using a simple model that treated magnet cross-section as a structure with several uniform cylindrical layers of different stiffness. More elaborated modeling based on FEA gives some increase of these numbers. Nevertheless, for all the designs, stresses in coil are still much less than the threshold value of 150 MPa when Nb_3Sn strand critical current degradation becomes significant and irreversible.

Table 4. Coil Stress Distribution.

Design / cable type	50 mm Type 1	45 mm Type 1	40 mm Type 1	40 mm Type 2
	Forces in coil @ 11T (kN/m)			
Fx	2590	2460	1870	2200
Fy	-940	-850	-710	-770
	Azimuthal stress at 11 T & 4.2 K (MPa)			
Inner layer	77	64	60	48.5
Outer layer	70	74	70	65.3

Table 5 presents calculated geometrical harmonics for magnet designs shown in figure 1. All harmonics here and below are reported at 10 mm reference radius. For each case it was possible to find a design solution with quite good field quality that was on the level of field quality requirements for SSC dipole magnets [9].

Table 5. Geometrical Harmonics.

Design version	50 mm Type 1	45 mm Type 1	40 mm Type 1	40 mm Type 2
b3	0.000	0.000	-0.003	-0.004
b5	-0.001	-0.000	0.008	0.026
b7	0.012	-0.001	0.012	0.036
b9	-0.072	-0.073	-0.255	-0.172
b11	0.027	0.073	0.232	0.167

Figure 2 shows sensitivity of magnetic field harmonics to random ±50-μm coil block displacements in the azimuthal direction. The SSC dipole specification data are shown at the same plot for comparison. The sensitivity of field harmonics to block displacemets grows as bore diameter decreases, but it is still below SSC requirements for harmonic RMS spread.

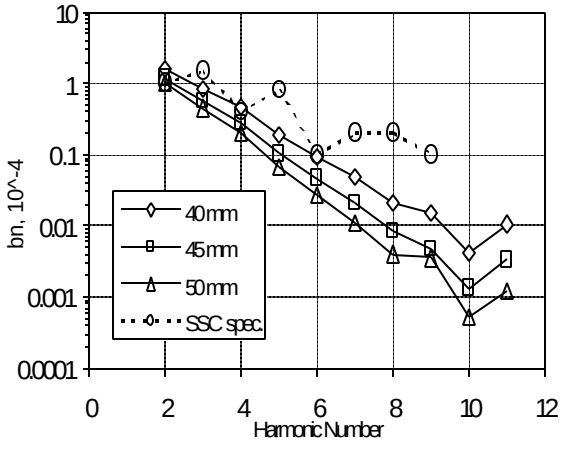

Fig. 2. Sensitivity of field harmonics to random coil block displacements.

Persistent currents induced in Nb_3Sn filaments during coil excitation result in significant change of low-order harmonics. This effect depends strongly on the effective filament diameter, which is a function of strand production technology. It can vary for Nb_3Sn strand from 50 μm to 150 μm. Calculations of persistent current contribution to the low-order field harmonics was done for the effective filament diameter of 70 μm. The results for the sextupole component are shown in the Figire 3 for three magnet designs that use the type 1 cable.

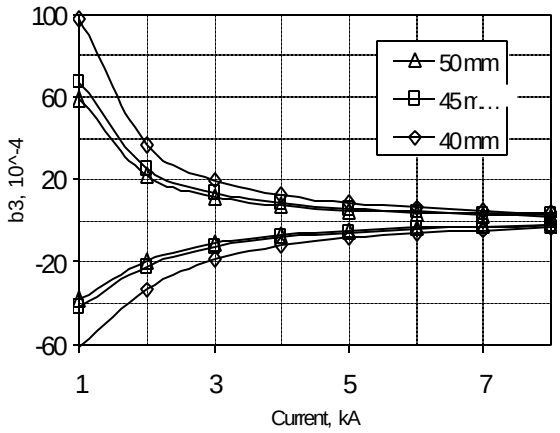

Fig. 3. Persistent current effects.

It is clear from this chart that persistent current induced sextupole component is quite large at injection for this value of effective filament diameter in Nb_3Sn strands. The effect is stronger for smaller bore diameter because the source of the field becomes closer to beam area. This result clearly indicates that if we are going to use Nb_3Sn strand to build magnets for a next generation collider, effective filament diameter must be reduced to 10-20 *m*m .

IV IRON YOKE EFFECTS

There are two major effects related to iron yoke saturation. They are:

- transfer function reduction,
- sextupole variation during excitation.

These effects can be observed even with infinite yoke outer diameter, when transfer function reduction is about 10%. An additional transfer function drop should be considered if the outer diameter is not large enough for the total magnetic flux screening. Figure 4 shows the transfer function and magnet fringe field change versus iron yoke outer diameter for the three cross-sections that use the type 1 cable. Curves 1, 2, and 3 represent the magnet fringe field and curves 4, 5, and 6 show transfer function change for the magnets with bore diameter of 50, 45, and 40 mm respectively at the 11 T central field. One can see that if fringe field is low enough, magnet transfer function remains constant and independent on the iron yoke outer diameter. To restrict the fringe field level by 100 Gs, one needs to have yoke outer diameter of 52 cm for 50-mm

bore design, 50 cm for 45-mm bore and 45 cm for 40-mm bore. It suggests significant material and cost savings if one choose smaller magnet bore diameter.

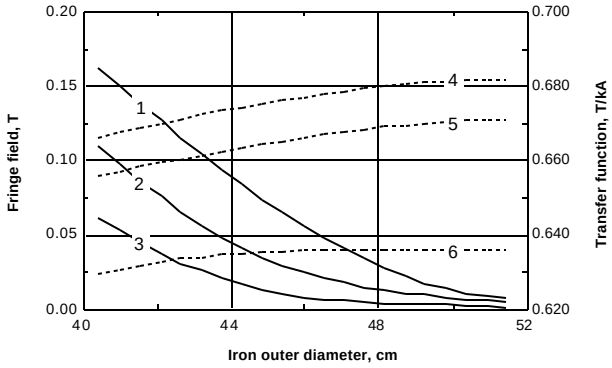

Fig. 4. Nonlinear Magnet Excitation Effects.

Sextupole behavior induced by iron yoke saturation, which is a well known effect, does not change much if one changes yoke outer diameter, although one can notice an earlier saturation of the yoke central region if smaller yoke diameter is used. Usual technique to correct this sextupole behavior is to introduce some obstacles to the magnetic flux in form of holes inside the yoke. The number, size, and location of the holes should be chosen and optimized to compensate for this iron saturation effect [10].

V SUMMARY

Several magnet designs with different Nb_3Sn cable types and bore diameters have been investigated. The magnetic analysis has shown that there was a good reason to reduce magnet bore diameter in order to gain in stress distribution, stored energy, and inductance. Although it was possible to find the 30-mm and 35-mm bore magnet cross-section versions with rather good field quality, cable block positioning for these cross-sections did not allow us to include them into our choice list. On the other hand, persistent current study results show some benefits of larger bore. Linear and non-linear iron induced effects did not add any severe restrictions to limit our cross-section choice, although smaller diameter would help to reduce magnet weight and cost.

Considering all the pros and cons above, the final cross-section choice was made to significantly simplify the problem of fabrication tooling development. It appeared possible to use part of equipment for the LHC high gradient quadrupole production at FNAL if bore diameter was less then 44.5 mm, insulation thickness was 0.125 mm, and type 1 cable was used [11]. To make coil robust and reliable, thicker cable insulation was chosen (0.25 mm). This choice has resulted in 43.5-mm bore diameter for the final cross-section choice.

To use the HGQ skin and skin contact tooling, the 400-mm outer yoke diameter was chosen although a significant fringe field with this choice could be expected. All magnetic design details can be found in [10-12]. Design of the Nb_3Sn dipole and production tooling is now in progress at Fermilab.

ACKNOWLEDGEMENTS

The work was performed in the frame of High Field Magnet R&D program at FNAL. Work was supported by the U.S. Department of Energy.

REFERENCES

[1] G. Dugan, "Really Large Hadron Colliders", 1996 Snowmass Workshop, proc., v. 1, pp. 90-100. Colorado, June, 1996.

[2] P. Cruikshank, et.al, "Mechanical Design Aspects of the LHC Beam Screen", LHC Project Report 128, July, 1997.

[3] A. Asner, R. Perin, S. Wegner, F. Zerobin, "First Nb_3Sn, 1m Long Superconducting Dipole Model Magnets for LHC break the 10 Tesla Field Threshold", CERN SPS 899-27 EMA.

[4] A. den Ouden, et al, "An Experimental 11.5 T Nb_3Sn LHC Type of Dipole Magnet" IEEE Trans. on Magn., vol. 30, NO.4, pp. 2320 - 2323, July, 1994.

[5] D. Dell'Orco, R. Scanlan, C.E. Taylor, "Design of the Nb_3Sn Dipole D20", IEEE Trans.on Applied Supercond., vol. 3, NO.1, March 1993.

[6] E. Gregory and T. Pyon, "Some Recent Developments in Low Temperature Superconductors for Fusion, High Energy Physics and Other Applications", Proc. of ICEC'17, Bournemouth (UK), 1998, p.339.

[7] D.R. Chichili, at al, "Niobium-Tin Magnet Technology Development at Fermilab", PAC-99, New-York, March 1999[8] Conceptual Design of the Superconducting Super Collider, SSC-SR-2020, March 1986.

[8] S. Russenchuck, " A Computer Program for the Design of Superconducting Accelerator Magnets" CERN AC/95-05 (MA), September 1995.

[9] Conceptual Design of the Superconducting Super Collider, SSC-SR-2020, March 1986.

[10] G. Ambrosio, et.al, "Magnetic Design of the Fermilab 11 T Nb_3Sn Short Dipole Model ", This conference.

[11] G. Ambrosio, et.al, "Conceptual Design of the Fermilab Nb_3Sn High Field Dipole Model", PAC-99, New-York, March 1999.

[12] G. Ambrosio, et.al, "Development of the 11 T Nb_3Sn Dipole Model at Fermilab" This conference.